model most frequently used when implementing structural analyses with material nonlinearity.

Generally then the calculation codes available today allow the user to define the $\sigma - \varepsilon$ curve by points, giving in this way the possibility to represent even very articulated stress-strain laws, as we will see later.

In § 13.1 we have mentioned the possibility to exploit this effect to increase the yield strength of the material, provided we can manage in some way the residual deformations; in fact from figure 13.20 it is clear that $\sigma_{Yld2} > \sigma_{Yld1} > \sigma_{Yld}$: if the final machining operations on the component (let's say a shaft, i.e. a cylinder) are performed after the pre-stress operations, then the permanent

Figure 13.20. σ–ε diagram for a material with bilinear behavior. Once σ_{Yld1} is reached above the elastic limit, the specimen exhibits residual strain ε_l upon unloading. At this point any load below σ_{Yld1} causes the material to work elastically, but deformation ε_l remains. Exceeding σ_{Yld1} results in an increase of residual strain.

deformations are "cancelled", so to say. Clearly with this operation the elastic limit is approached to the ultimate limit, thus making the component less resilient, i.e. more brittle.
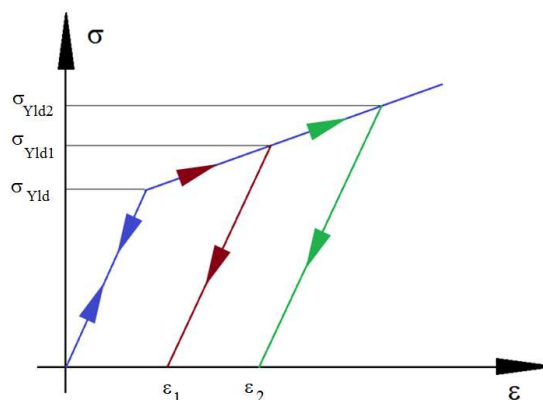
13.4   Beam in torsion beyond the elastic limit

And since we've been talking about circular sections, an analogous speech to that made for a beam subjected to a pure bending moment can be repeated for a beam subjected to pure torsion. To simplify the theoretical calculation we will use a solid circular section bar with diameter d = 40 mm and length L = 100 mm (actually the length does not have much importance, since the stress depends only on the diameter and the applied torque). Figure 13.21 shows the model made with 8-node brick elements of one quarter of the bar. The structure is doubly symmetrical, but the load is not. It is therefore essential to apply anti-symmetry constraints to the nodes lying in the symmetry planes (see Chapter 2). The surface at one end of the beam is clamped to ground, while at the other end the torque (a quarter of the total value, since we are analyzing a quarter of the structure!) is applied through a spider of rigid MPC elements. As in the case of bending, through Solid Mechanics relationships we are able to calculate what is the torque that causes the skin fibers to yield.If we suppose to employ the same material used previously (i.e. with σ_{YLd} equal to 290 MPa) we know that the corresponding shear stress is worth (it's easy to derive the following relation thinking about the Von Mises equation, which links σ and τ):

$$\tau_{Yld} = \frac{\sigma_{Yld}}{\sqrt{3}} = 167.4 \, \text{MPa}$$

Therefore, being $\tau = \frac{16 \cdot M_t}{\pi \cdot d^3}$, it is immediate to derive $M_t = 2104007$ Nmm.

Let's set this value aside for the moment. We will need it later to calculate the plastic torsion margin for a solid circular section.

Now, similarly to the case of bending, let's calculate the magnitude of the torque that makes a circular crown of 10 mm thickness plasticize. In other words, the core having a diameter $d_1 = 20$ mm will continue to work in the elastic field, while the outer crown will be totally plasticized. We will have the situation shown in figure 13.22.
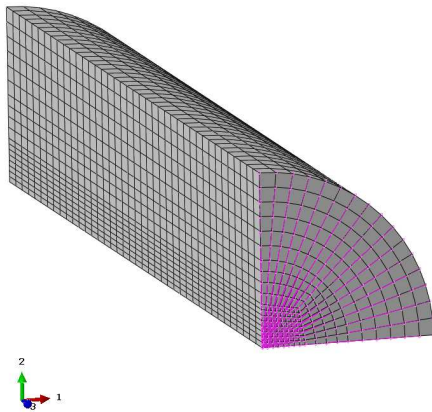

Figure 13.21. Model of a quarter bar subjected to pure torsion. Appropriate antisymmetry constraints were applied.
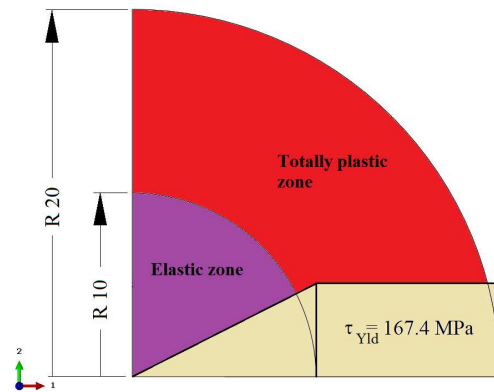
Figure 13.22. Distribution of shear stresses.

Once we have determined the value of this torque we will apply it to the finite element model. Keeping in mind figure 13.22 and knowing that the τ act on elementary areas $da = r \cdot d\vartheta \cdot dr$ we can write:

$$M_{tpl} = \frac{\pi \cdot d_1^3 \cdot \tau_{Yld}}{16} + \int_0^{2\pi} \int_{r_1}^{r} \tau_{Yld} \cdot r \cdot da \qquad (13.1)$$

By carrying out the double integral and the other operations we get:

$$M_{tpl} = 2710671 \, \text{Nmm}$$

Figure 13.23 shows the contour of the shear stress and its trend as a function of radius (along the line shown) when the torque just calculated is applied. The shear stress is expressed in a cylindrical reference system with the origin in the center of the bar

and with the z-axis directed as the axis of the bar itself. In particular, the plotted τ is τ_{23}, which represents $\tau_{z\theta}$.
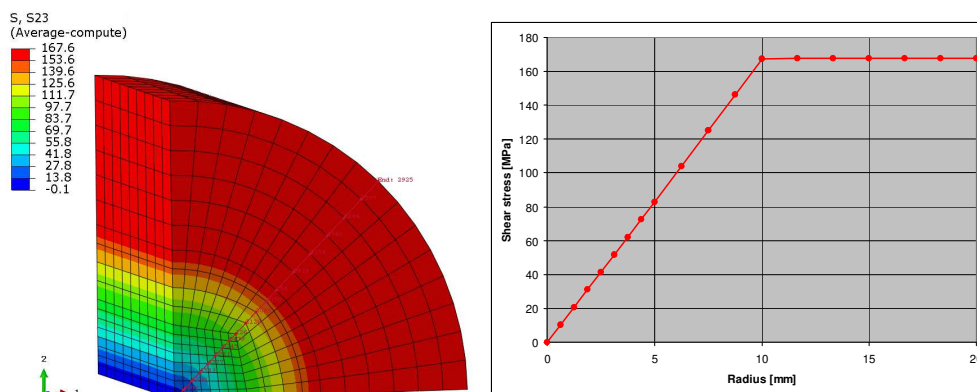

Figure 13.23. Shear stress. Since there are no other stress components, even in this case (as for the deflected beam with the plane stress model) it is possible to study directly the shear stress because this will be the only one to contribute to the Von Mises stress.

Finally, figure 13.24 shows information about the residual shear stresses once the torque has been "released" in a subsequent load step.

At this point, as we have done in the case of bending, we can calculate the coefficient of plastic collaboration. To do this, it is necessary to determine the torque that plasticizes 100% of the section. It is possible to do this using (13.1), keeping in mind that the first term (representing the triangular stress distribution) will be zero and that the extremes of integration along the radius will be different.
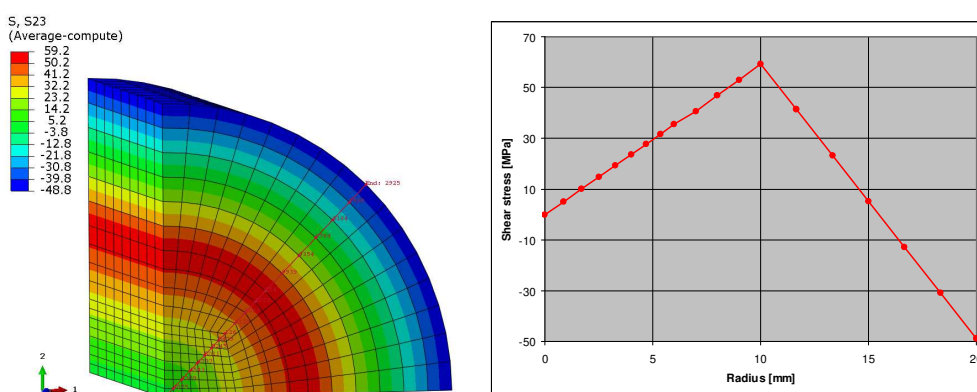

Figure 13.24. Residual shear stress.

We will have:

$$M_{tpl100\%} = \int_0^{2\pi} \int_0^r \tau_{Sn} \cdot r \cdot da$$

By solving the double integral we get $M_{tpl100\%} = \dfrac{\tau_{Yld} \cdot \pi \cdot d^3}{12} = 2798112\,\text{Nmm}$.

Therefore, the coefficient of plastic torsion collaboration for the circular section holds:

$$C_{plt} = \frac{M_{tpl100\%}}{M_t} = \frac{2798112}{2098584} = 1.\overline{33}$$

This value is identical to the theoretical value [1]. In this case, unfortunately, the calculation for total plasticization fails even if a rotation is applied instead of a torque; the problem lies in the outermost elements that undergo too much deformation and prevent the solution from reaching convergence.

13.5 Industry practice

13.5.1 Drive shafts for racing car

In the previous paragraphs, we have repeatedly mentioned a drive shaft for a racing car. Let's see then what are the advantages of pre-plasticizing such a component. In figure 13.25 we show a 120° portion of the model, moreover cut with a plane in correspondence of the centerline; we will therefore need to introduce anti-symmetry constraints, since we are going to apply a torque.
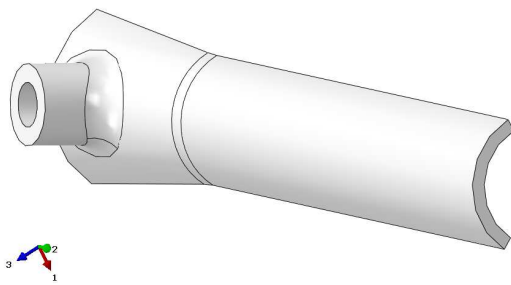

Figure 13.25. CAD model of a drive shaft for an open wheel racing car. Given the axial symmetry (120°) and with respect to the length, we study only a sixth of it with the appropriate symmetry and anti-symmetry constraints.
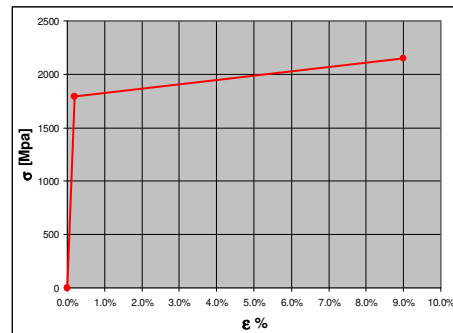
Figure 13.26. Bilinear σ–ε diagram for the material being used (NC310YW): σ_{Rp02} = 1790 MPa, σ_{Rt} = 2150 MPa and A% = 9%.

The section we are interested in is the central one, with an external diameter of 40 mm and a thickness of 3.5 mm. The peak torque, measured several times with telemet-